An Analytical Approach to Predict Cohesion and Interfacial Failures of CFRP/Steel Composites Under Prolonged Exposure to Aqueous Solutions

Article *in* Case Studies in Construction Materials · February 2022

DOI: 10.1016/j.cscm.2022.e00949

CITATIONS
4

READS
100

3 authors:

Nirosha Dilrangi Perera
Sri Lanka Technological Campus
10 PUBLICATIONS **10** CITATIONS
SEE PROFILE

Tharika Kahandawaarachchi
Western Sydney University
10 PUBLICATIONS **18** CITATIONS
SEE PROFILE

JCPH Gamage
University of Moratuwa
75 PUBLICATIONS **641** CITATIONS
SEE PROFILE

Case Studies in Construction Materials 16 (2022) e00949

Contents lists available at ScienceDirect

Case Studies in Construction Materials

journal homepage: www.elsevier.com/locate/cscm

Case study

An analytical approach to predict cohesion and interfacial failures of CFRP/steel composites under prolonged exposure to aqueous solutions

U.N.D. Perera [a], K.A.D.Y.T. Kahandawa Arachchi [b,*], J.C.P.H. Gamage [b]

[a] Lecturer, Sri Lanka Technological Campus, Padukka, Sri Lanka
[b] Department of Civil Engineering, University of Moratuwa, Sri Lanka

ARTICLE INFO

Keywords:
CFRP/steel joints
Moisture effect
Analytical model
Adhesive degradation
Interface degradation
Bond

ABSTRACT

The long-term performance of Carbon Fibre Reinforced Polymer (CFRP) strengthened steel joint under prolonged exposure to moisture conditions is imperative in the applications of structures exposed to groundwater or seawater. Analytical models to determine the bond characteristics of CFRP/steel composites subjected to prolonged exposure in aqueous solutions are yet to be explored. This paper explores the cohesive and interfacial failure parameters of such CFRP/Steel composites theoretically. Thirty double-strap joints and twenty adhesive coupons were tested to determine the residual strength after exposure to seawater and distilled water for 6 and 12 months. An analytical model was developed to determine the degradation of adhesive material, bond and the interfaces of composite exposed to seawater and distilled water. The developed model is in good agreement with test results and capable of predicting initial bond degradation rate and stabilized degradation under-considered exposure conditions. Furthermore, the model could predict the contribution from the interfaces, bond line, and adhesive component on the degradation of composite in service.

1. Introduction

With a majority of the existing steel structures in the world reaching their serviceability life spans, retrofitting steel structures have become a popular focus in the construction sector [1–3]. In that case, Carbon Fiber Reinforced Polymers (CFRP) pioneer the trends in retrofitting materials when it comes to steel structural elements [1,4,5]. Their lightweight, high strength: weight ratio and corrosion resistance make them an excellent candidate for retrofitting deteriorated steel structures [6].

Nevertheless, structural steel elements are often exposed to harsh environmental conditions which hinders the performance of the retrofitting material as well [1,7]. Even though CFRP itself could exhibit excellent materials properties, when met with harsh conditions, the adhesive used in bonding the CFRP to the steel surface exhibits adverse reactions. The chemical performance of the adhesive was found to be severely reduced when exposed to aqueous solutions [8]. Moisture intrusion into the FRP/steel bonded joints occurs as a result of diffusion through the adhesive or adherend, wicking along with the interface or by capillary action [9]. Zhou et al. [10] pointed out that the water molecule entering an epoxy resin could be either (a) joining with the hydrophilic molecules in the resin, (b) occupying free spaces in the resin or (c) bulk dissolution into the polymer would occur according to several studies. The water

* Corresponding author.
E-mail address: tharikakahandawa@gmail.com (K.A.D.Y.T. Kahandawa Arachchi).

https://doi.org/10.1016/j.cscm.2022.e00949
Received 22 October 2021; Received in revised form 1 February 2022; Accepted 13 February 2022
Available online 19 February 2022

ingress into the bond line will result in the weaker secondary Van der Waals forces at the steel/epoxy interface and hence result in debonding failure of the composite [11]. In a recent review by Li et al. [12], chlorine ingression into the adhesive when exposed to seawater conditions was found to be damaging the interface molecular structure of the adhesive and hence degrading the tensile performance of the adhesive. Furthermore, the experimental results of Nguyen [13] revealed that the strength and stiffness of a CFRP bonded steel joint are mostly dependent on the change of adhesive properties when continuously exposed to seawater. They further noted that the degradation is at its peak at the early age of the exposure condition at 20 °C. In the experiments of Heshmati et al. [14] almost 50% reduction of the strength was noted in the specimens exposed to seawater conditions which they claim to be correlated with the loss of adhesive ductility when subjected to wet and dry conditioning. Thereby, the degradation of adhesive properties when subjected to sea water conditions should be expected and hence the failure modes of the composites should change accordingly.

According to Pang et al. [15] and Borrie et al. [16], there are six modes of failure when it comes to CFRP/Steel composites. (a) Steel yielding (b) adhesion failure at the steel/adhesive interface, (c) cohesive failure in adhesive, (d) adhesion failure at the adhesive/CFRP interface, (e) CFRP delamination failure, and (f) CFRP rupture. Heshmati et al. [8] noted the failure mode of the CFRP/Steel interface to be shifting from cohesive failure to interlaminar failure when exposed to seawater wet and dry conditions. This hypothesis was supported by the review conducted by Li et al. [12] which also suggests that the failure mode would shift from cohesive failure to interlaminar failure when exposed to NaCl solutions.

It should be further elaborated that the surface wettability of steel would directly affect the moisture intrusion into the composite. The surface roughness of the steel substrate would directly influence the wettability of steel as well as the bond performance of CFRP [17,18]. In that case, Sajid et al. [17] stipulate that the smoother the surface of the steel is, the more hydrophobic it becomes. The experimental results of both Silva et al. [19] and Russian et al. [20] suggest that when the surface roughness of the comprising material interface is decreased, the strength parameters of the composite increase due to enhanced interface properties. Thereby, the surface preparation conditions of the steel substrate can be established as a vital parameter in the study. Teng et al. [21] suggest that three surface parameters; surface energy, chemical composition and surface roughness would affect the quality of adhesion between the steel and the CFRP substrate. In this case, the surface energy of the composite refers to the “excess energy” stored at the surface of the substrate due to the creation of the surface itself. Chemical composition refers to the chemical activeness of the surface which is free of contaminants for better bond performance [16].

Since conducting experimental studies to evaluate the long-term performance is time-consuming and resource-intensive, the development of analytical models may help designers to identify the bond strength performance and detail the composite to maximize the service performance of structural thin-walled composite members. Such available theoretical models are summarized in a recent study by da Silva et al. [22]. These analyses are developed for single and double lap joints and are capable of considering the linear and non-linear behaviour of adhesives and adherents in two-dimensional (2D) and Three-dimensional (3D) scenarios [22]. Among these, the Hart-smith model is often used and known to predict accurate results in the CFRP/steel joints made of ductile adhesives and elastic adherents [23].

Although several studies have investigated an experimental approach towards prolonged exposure of CFRP/Steel composites in aqueous solutions like seawater and cohesive failure behaviour, a limited number of studies have been focused on a theoretical approach to predict the bond properties when the composite stimulates both adhesive degradation (cohesive failure) and steel-adhesive interface degradation (interfacial failure) conditions combinedly as per authors’ knowledge. A majority of the previous studies had been focused on the cohesive failure mode, whereas the theoretical approach explored in this research aims to expand the knowledge on CFRP/Steel bond performance at prolonged environmental conditions by including the interfacial parameters to the equation.

2. Test program

Thirty double strap joints were prepared. The summary of the specimen details is listed in Table 1. In addition, twenty adhesive coupon tests were also carried out to determine the adhesive degradation behaviour with long term conditioning.

2.1. Material properties

5 mm thick steel plates were used to prepare the double strap joints. The normal modulus, unidirectional CFRP sheets [24] and a two-part epoxy adhesive [25] were used for strengthening. The mechanical properties of both adhesive and adherents were tested in accordance with the ASTM standards [26–28]. The test configuration and measured properties are shown in Table 2 and Fig. 1.

Table 1
The summary of the specimen details.

Environmental exposure condition	Exposure duration (Months)	No. of specimens tested
Unconditioned (Control)	0	6
Prolonged exposure to 5% NaCl solution (SW)	6	4
	12	4
Prolonged exposure to distilled water (DW)	6	4
	12	4
5% NaCl solution and Wet/Dry Cyclic condition (AC)	6	4
	12	4

The fabrication of adhesive coupons was carried out as per ASTM D 638 test standards. Type II [26] coupons with a thickness of 7 mm were used and moulds cut into a thin aluminium sheet was used to obtain the sample as per the standard specifications. In order to take the time-dependent adhesive properties, material testing was done at 6 months and 12 months of exposure durations for SW and DW conditions. This was done with a total of 20 adhesive coupon specimens and the test results are discussed in Section 3.1.

2.2. CFRP/Steel double strap joint preparation and conditioning

A schematic diagram of a double strap joint specimen is shown in Fig. 2. The lengths L_1 and L_2 were chosen by a test series carried out to determine the effective bond length of CFRP/steel joints by Chandrathilaka et al. [1]. According to the test results, the minimum required bond length was identified to be 110 mm [1]. Furthermore, it was decided to use unequal lengths for L_1 and L_2 to eliminate the uncertainty of the debonding location which is a popular trend in literature [7,29]. This way, instead of monitoring the whole sample, the shorter length side will be focused and observed [7]. Hence, L_1 and L_2 were chosen as 115 mm and 120 mm, respectively, where both are higher than 110 mm and one side shorter.

Surface preparation was carried out by grinding the surface using a grinder and adopting a primer coating to obtain an even surface. The wet-lay-up method [30] was followed to attach the CFRP sheet to the steel joint [31]. For the wet-lay-up method, first, a primer was applied to the sample surface. Then the two-part epoxy resin was mixed and the CFRP sheet was impregnated with the resin before applying to the surface. Next, the CFRP sheet was carefully placed on the prepared sample and evened out using a spatula. The samples were cured for 7 days at room temperature (28 °C) before environmental conditioning. Strain gauges were also attached to the CFRP layer surface at 35 mm and 90 mm from the loaded edge to monitor the strain variation of each joint (Fig. 2(b)). It is worth noting that the gauges were placed on the shorter bond length (L_1) side which will be closely monitored.

Three different exposure conditions; (a) prolonged exposure to seawater (SW), (b) dry/wet exposure to seawater (AC) and (c) prolonged exposure to distilled water (DW) were considered. The seawater condition was simulated by adding 5% NaCl to the distilled water by weight. The dry/wet exposure was achieved by immersing test samples in the 5% NaCl solution for 2 months and keeping them in a dry-indoor environment for the next 2 months. The exposure periods of 6 and 12 months were considered for all the above conditions. At the end of the exposure period, the bond strength was determined at ambient conditions (Fig. 3). The load and strain measurements were monitored during testing.

3. Test results

The performance of a composite joint depends on the behaviour of individual materials and interfaces between the substrates. Hence, the results presented here are in terms of both material and interfacial degradation caused due to moisture ingression.

3.1. Material degradation

The moisture intrusion affects the strength depletion of bonded joints as well as the individual joint components. The adhesive material and the CFRP resin tend to degrade at a higher rate, compared to the Carbon fibres or the steel substrates. Since no signs of fibre rupturing were seen in the failed specimens, a lower rate of CFRP material degradation can be assumed at all exposure conditions in the current study. This assumption had been validated by previous studies for the exposure duration of 360 days [13,14]. Hence, the adhesive strength degradation was considered as the key issue.

3.1.1. Adhesive strength degradation

Fig. 4(a) & (b) show the degradation of tensile strength and E-modulus of the adhesive material subjected to prolonged exposure to seawater and distilled water for 12 months. Experimental adhesive strength results under seawater immersion were compared with the results obtained by Nguyen et al. [13]. Since the results by Nguyen et al. [13] were obtained for a different temperature level (i.e. 20 °C), a theoretical model was used to calculate the adhesive strength degradation rate (k) at the temperature level considered in the present study (i.e. 28 °C – room temperature). The Arrhenius equation is used as a formula for the temperature dependence of reaction rates. The modified version of the equation was considered and adjusted accordingly. This was assuming that the two adhesive strength degradation rates at 28 °C and 20 °C are k_1 and k_2 respectively.

$$k1 = k2 * \exp (Ed / R) * (T2–1 – T1–1) = - 0.0035126$$

Where,

Table 2
Measured mechanical properties of the materials at ambient conditions.

Mechanical property	Adhesive	CFRP	Steel
Average Ultimate Strain	0.012	0.009	0.007
Average Ultimate Tensile Strength (MPa)	24.10	1575.00	583.00
Average Yield Tensile Strength (MPa)	–	–	512.00
Average Modulus of Elasticity (Along fiber direction) (GPa)	1.900	175.60	206.30

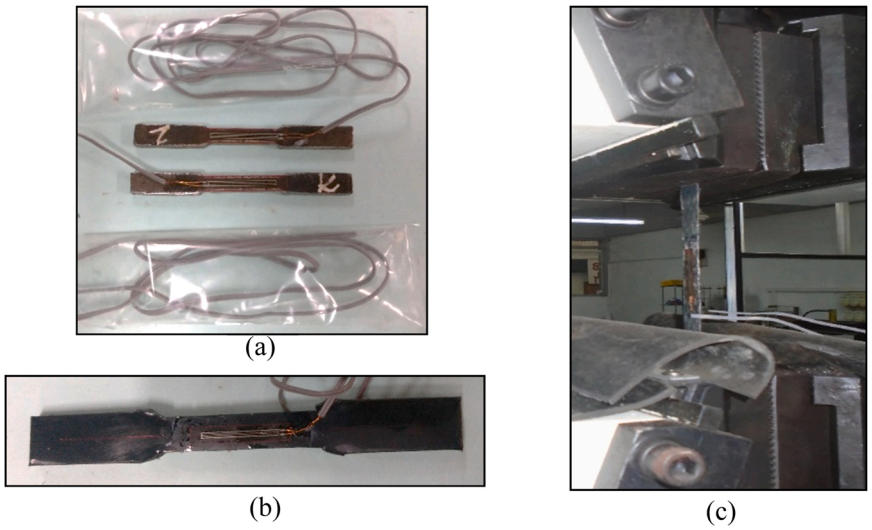

Fig. 1. Test coupons: (a) Steel (b) Adhesive (c) CFRP sheet.

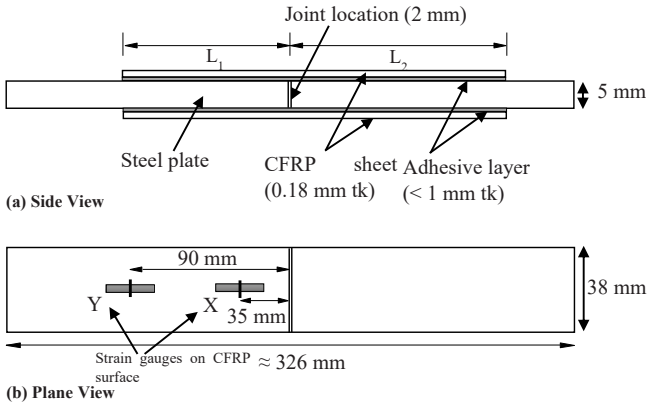

Fig. 2. (a) A schematic diagram of double strap joint (b) Sample specimen.

- k_2 is −0.0021 per day [13],
- E_d is the activation energy or the minimum energy required for moisture diffusion (47.15 kJ/mol K),
- R is the universal gas constant (8.3143 J/mol K),
- T_2 is the exposure temperature of the study by Nguyen et al. in Kelvin (293 K)
- T_1 is the exposure temperature of the present study in Kelvin (301 K)

A similar E_d value had obtained from a past study [32] and it can be experimentally determined using the Arrhenius type equation and moisture diffusion data [32].

Then, the adhesive strength degradation behaviour over time was obtained using the following Phani and Bose model equation [33]:

$$\sigma_{t,a}(t) = (\sigma_{(o)} - \sigma_{(\infty)}) \exp(k^*t) + \sigma_{(\infty)}$$

Where,

- $\sigma_{t,a}(t)$ is the adhesive tensile strength after the exposure duration "t",
- $\sigma_{(o)}$ is the adhesive strength at ambient conditions (100%)
- $\sigma_{(\infty)}$ is the ultimate asymptotic adhesive strength in moisture (62%) [13]
- k is the adhesive strength degradation rate
- t is the exposure duration considered

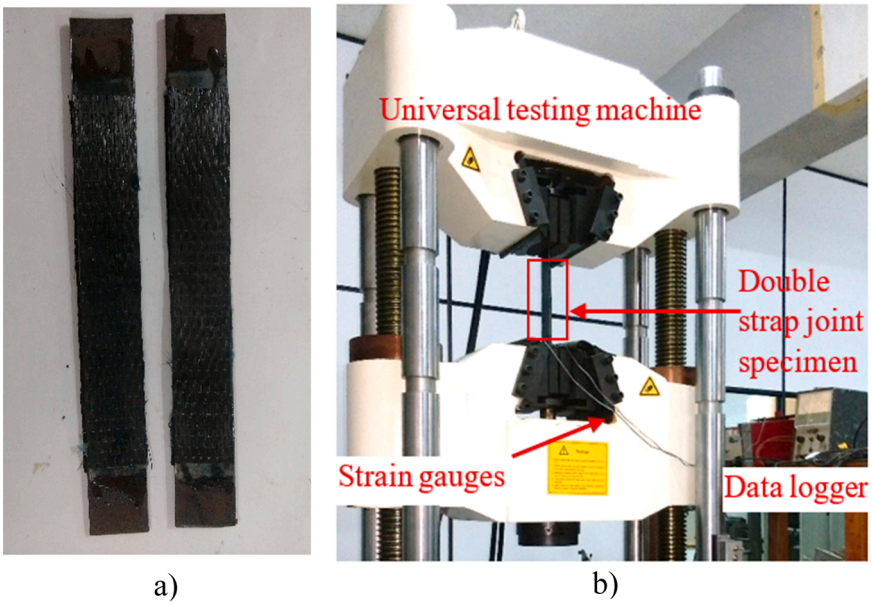

Fig. 3. a) Sample specimen b) Test set up and instrumentation.

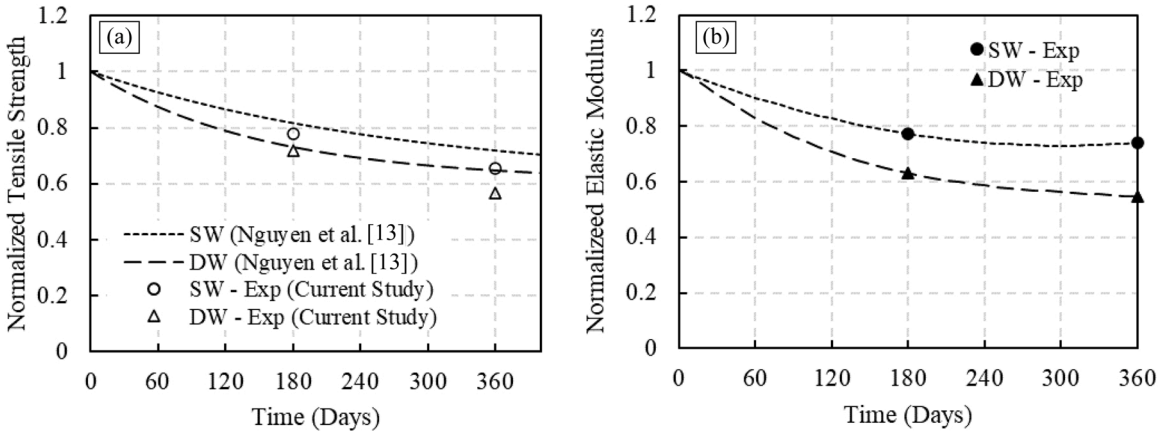

Fig. 4. Normalized degradation behaviour of mechanical properties of adhesive in sea water and distilled water at ambient temperature (a) Tensile Strength (ft,a) (b) Elastic modulus (Ea).

The model predicted adhesive strength degradation plot is well-compared with the experimental results in Fig. 4(a). It is noted that the rate of degradation of the adhesive mechanical properties is higher in the DW condition compared to the SW condition [14]. Even though the adhesive tensile strength degradation is somewhat similar, Elastic moduli have a comparative difference between both conditions. This may be due to the different moisture absorption rates in seawater and distilled water exposures.

3.2. CFRP/steel bond degradation

3.2.1. Failure mechanism

The failure mode of the unconditioned (control) samples showed a combined behaviour of cohesive failure and interfacial failure modes (Fig. 5). Long-term exposure to the simulated seawater tended to change the failure mode completely towards an interfacial failure mode. This implies that the rate of degradation of the interfacial bond performance in the surface between steel and the adhesive is higher when compared to the individual degradation rate of the adhesive or the CFRP material. Several research studies have witnessed a similar change in the failure mode of the long-term exposed specimens, i.e. a shift from cohesive failure (adhesive failure) to interface failure, due to moisture ingression into the interface [11]. However, some studies also observed no change in the mode of failure which remained to be a cohesive type in both control and conditioned samples [13]. Studying the effects of the exposure condition on the adhesive degradation solely revealed the joint strength degradation behaviour of such situations.

Fig. 5. Failure modes of the specimens: a) Distilled water at ambient temperature (Ave. 28 °C)/Conditioning period - 6 months b) Distilled water at ambient temperature (Ave. 28 °C)/Conditioning period - 12 months c) Simulated seawater (5% NaCl) at ambient temperature/Conditioning period – 6 months d) Simulated seawater (5% NaCl) at ambient temperature/ Conditioning period - 12 months e) Dry /wet cyclic condition in simulated seawater – 5% NaCl at ambient temperature/ Conditioning period - 6 months f) Dry /wet cyclic condition in simulated seawater – 5% NaCl at ambient temperature/ Conditioning period - 12 months.

All the specimens showed a discolouration when the samples were removed from the immersion basin, which occurred due to the accumulation of corrosion products. This was noticeable even after 6 months of the exposure period and the extent of the discolouration had increased in the following 6 months. Except for the specimens submerged in a simulated seawater bath, all other specimens showed corroded edges on the bonded region. This was significantly observed in dry/wet cyclic conditions and almost 50% of the surface was covered with rust after 12 months of the exposure period (Fig. 5). Remarkably, the continuous exposure to seawater showed a clearer surface in the bonded area compared to other samples (Fig. 5). This can be attributed to the fact that the larger molecular size of saltwater decelerates the moisture diffusion to the bond through the outside adherend or wicking. When the joints were exposed to a dry condition after saltwater immersion, condensed salt particles get accumulated on the joint and accelerated the corrosion process in the following wet period. Thus, the wet/dry cycles caused an adverse condition for the durability of the bonded joint and precautions should be taken like applying silane coupling agents [11] to prevent the interfaces from damage. However, since the corrosion was seen on the edges of steel plates, moisture ingression to the joint in the current study was mostly due to the wicking along the interface.

3.2.2. Bond strength and strain variation of double strap joints

Fig. 6 shows the residual bond strength capacities of the conditioned specimens in 6 months and 12 months of exposure durations. In 6 months, the bond strength degradation of both DW and SW samples was about 28%. This implies a similar rate of interfacial degradation in both conditions irrespective of the alkalinity percentage in the water. Further, if the outliers were disregarded, the variation in the joint failure load followed the adhesive degradation rate in DW condition as shown in Fig. 4. This implies that at the early age of exposure duration, the degradation rates of adhesive and the interfacial fracture energy due to moisture is similar. Within

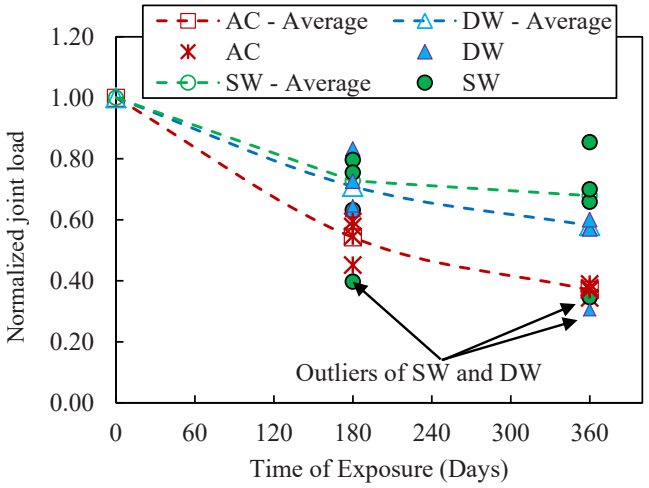

Fig. 6. Bond strength degradation of CFRP/steel joints with exposure period.

the following 6 months, DW samples had lost a further 16% of their joint strength and SW samples showed a negligible variation. In the DW condition, moisture ingression continued, and it further degraded the interfacial properties. However, a decreased rate of reduction was observed. That must be due to the positive reinforcement of adhesive plasticization which allowed the adhesive to spread through the bond surface. The results of the SW condition confirmed that bond strength degradation is severe in the early ages as the first 6 months as observed by Nguyen et al. [13]. A negligible bond strength degradation was then followed may be due to the larger molecular size of saline water particles which hindered further ingression of moisture which clearly showed in the failed specimens.

The strain readings of the control specimens at 35 mm and 90 mm away from the joint showed decreased stress distribution further away from the joint (Fig. 7). A greater slope in the strain readings at location Y was observed with respect to the strain readings at X. After 12 months of exposure duration, DW samples showed a significantly lower yield point with strains less than 500 micro strains. Interestingly, strain readings of SW samples showed strain variation similar to each other at both X and Y locations.

AC samples had lost nearly 50% of their initial bond strength in 6 months. After 12 months of exposure duration, the bond strength had further reduced up to 63%. Since the interface degradation is more critical in the cyclic exposure to seawater, the lowest ultimate bond strength was achieved in AC specimens, as expected.

4. Theoretical modelling of long-term performance of CFRP/steel joints

The experimental results showed the adhesion failure modes as the dominant failure mode which implied the impact of both interface and adhesive degradation. The residual joint strengths in the adhesive failure mode (cohesive)were theoretically estimated using the available variation of material properties of the adhesive throughout the exposure period. The Hart-Smith (1973) model [34]

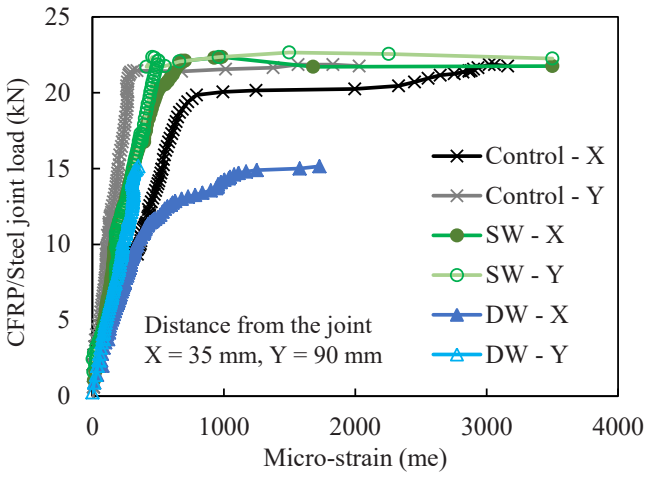

Fig. 7. Strain variation of CFRP/steel joints at 12 months of conditioning.

was used for this purpose. This model had been successfully used in the previous studies to predict the residual CFRP/steel joint capacities in both moisture environments and elevated temperatures [13,35]. Since it was developed considering the non-linearity of the adhesive, the model predicts the ultimate load of the joints which failed due to the depletion of the adhesive rather than the interfacial properties.

4.1. The time-dependent effective bond length

The maximum joint strength could be achieved only if the minimum bond length is provided in the double lap joint. Hart-Smith [34] suggested the following equation (Eq. 1) to predict the minimum lap length which can develop the maximum joint strength.

$$L_{min} = P / (2* \tau_f(t)) \quad (1)$$

Where P is the ultimate failure load per unit width of the joint and $\tau_f(t)$ is the adhesive shear strength. However, on account of long-term exposure conditions and possible imperfections in fabrication Hart-Smith introduced Eq. (2) to calculate the practical design lap length (L_{eff}) of a double lap joint.

$$Leff = \frac{\sigma_{ult}}{\tau_f(t)} \cdot t_i + \frac{2}{\lambda} \text{where} \lambda = \sqrt{\frac{G_a(t)}{t_a}\left(\frac{1}{E_o t_o} + \frac{2}{E_i t_i}\right)} \quad (2)$$

Where, σ_{ult} is the ultimate tensile strength of steel, $G_a(t)$is the shear modulus of the adhesive, E and t denote the elastic modulus and the thickness of the respective inside ($_i$)and outside ($_o$) adherents and t_a is the adhesive thickness. The adhesive shear strength parameters involved in this equation are time-dependent variables. The following Eqs. (3) and (4) [31]were used to determine these parameters with the available results of $\sigma_{t,a}(t)$ and $E_a(t)$ in Section 3.1.

$$G_a(t) = \frac{E_a(t)}{2(1+\nu)} \quad (3)$$

$$\tau_f(t) = 0.8\, \sigma_{t,a}(t) \quad (4)$$

Fig. 8 shows the variation in the required bond length with the exposure duration. The curves for L_{eff}(SW) and L_{eff}(DW) denote the theoretical bond lengths obtained from Eq. (2). As per these plots, the minimum effective bond length required at ambient conditions is 136 mm ($L_{eff\ (t=0)}$) theoretically whereas in this research it was found as 110 mm experimentally ($L_{min,\ Exp\ (t=0)}$). The 23% difference in the values must be taken into account for the tolerance provided in theory for fabrication considerations in the early age of exposures. The required time-dependent variation of the required bond length in the present study ($L_{min,exp}$) was then generated observing the trend of the model predicted curve (Fig. 8).

According to Fig. 8, the bond length requirement increases with the variation of adhesive shear parameters over time as depicted by Eq. 2. Thus, the lap length of the specimen should be initially designed with the maximum bond length requirement based on the exposure duration. In fact, the experimental determination of effective bond lengths for different exposure durations requires a higher resource allocation. Thus, based on the current study, the following relationships were derived for the practical design bond length required ($L_{eff,d}$) in double strap joints with CFRP sheets and manually ground steel surfaces when exposed to DW and SW conditions.

$$L_{eff,d\ (SW)} = L_{min,Exp} + \Delta L_{dur\ (SW)} + \Delta L_{dev} \quad (5)$$

$$L_{eff,d\ (DW)} = L_{min,Exp} + \Delta L_{dur\ (DW)} + \Delta L_{dev} \quad (6)$$

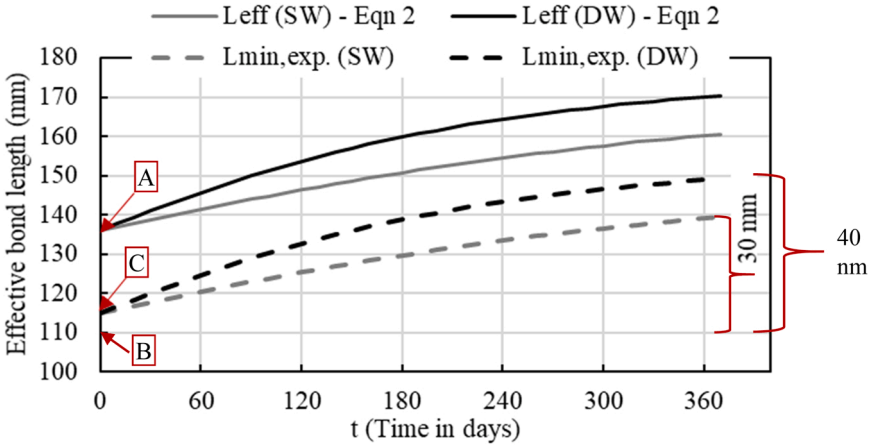

Fig. 8. Variation of effective bond length over time in DW and SW conditions (Points A, B and C refer to Leff(t = 0) = 136 mm, Lmin,Exp (t = 0)= 110 mm and Lprovided = 115 mm).

Where ΔL_{dur} is the additional bond length required due to the long-term exposure and ΔL_{dev} accommodates any deviations that might occur due to unexpected issues in joint fabrication.

Consider the graphs, $L_{min,exp\ (SW)}$ and $L_{min,exp\ (DW)}$ in Fig. 8. In both cases $L_{min,exp(t=0)}$ is 110 mm. In that case, ΔL_{dur} is the difference between the minimum and maximum points as shown in Fig. 7. ($\Delta L_{dur\ (SW)} = 30$ mm, $\Delta L_{dur\ (DW)} = 40$ mm). Since the adhesive mechanical properties are almost in an asymptotic state after the exposure to 12 months of duration, as shown in Fig. 4, a barrier of 10 mm would be sufficient for the future variation of material properties. A minimum of 10 mm allowance can be accommodated for $\Delta L_{dev.}$ Thus, the additional bond length required due to the long-term exposure to SW and DW conditions for more than 360 days were obtained as 40 mm (30 + 10 mm) and 50 mm (40 + 10 mm), respectively.

4.2. The joint strength degradation

The following Hart-Smith model equations (Eqs. 7 and 8) were considered to calculate the joint strength per unit width of the double-lap joints with a single layer of CFRP adherend.

$$Pi(t) = \sqrt{\left[2.\tau_f.t_a\left(0.5\,\gamma_e + \gamma_p\right).2.E_i.t_i\left(1 + \frac{E_i t_i}{2E_o t_o}\right)\right]}; \quad \text{where, } 2E_o t_o > E_i t_i \tag{7}$$

$$Po(t) = \sqrt{\left[2.\tau_f.t_a\left(0.5\,\gamma_e + \gamma_p\right).4.E_o.t_o\left(1 + \frac{2E_o t_o}{E_i t_i}\right)\right]}; \quad \text{where, } 2E_o t_o < E_i t_i \tag{8}$$

Where, γ_e and γ_p are the elastic and plastic adhesive strains, respectively and $P_i(t)$ /$P_o(t)$ refers to the ultimate load per unit width in the respective condition. E and t denote the elastic modulus and the thickness of the respective inside ($_i$)and outside ($_o$) adherents and t_a is the adhesive thickness. The unknown adhesive strain properties over time were calculated using the relationships as in [13,34].

$$\gamma_e(t) = \frac{\tau_f\ (t)}{G_a(t)} \tag{9}$$

$$\gamma_p(t) = 3\ \ \gamma_e(t) \tag{10}$$

In the current study, $2E_o t_o < E_i t_i$ and hence the Eq. (8) was used. The joint failure load P_{fail} was then achieved as recommended in the Hart-Smith model (Eq. 11 and 12). The width of the joint (b) is 38 mm.

If the bond length ($L_{provided}$) $< L_{eff}(t)$

$$P_{fail} = b.P_o(t).\left(L_{Provided}/L_{eff}\right) \tag{11}$$

Otherwise

$$P_{fail} = b.P_o(t) \tag{12}$$

Theoretically predicted bond strength capacities from the above equations were then compared with the experimental results for both SW and DW conditions (Fig. 9). These plots prove that a greater strength could be expected when the failure was merely due to the adhesive degradation being provided with better interfacial properties and adequate lap lengths. According to Fig. 9(b), the theoretical and experimental curves seem to be similar for the provided lap length, $L_{Provided}$. This implies the bond strength of CFRP/steel joints in

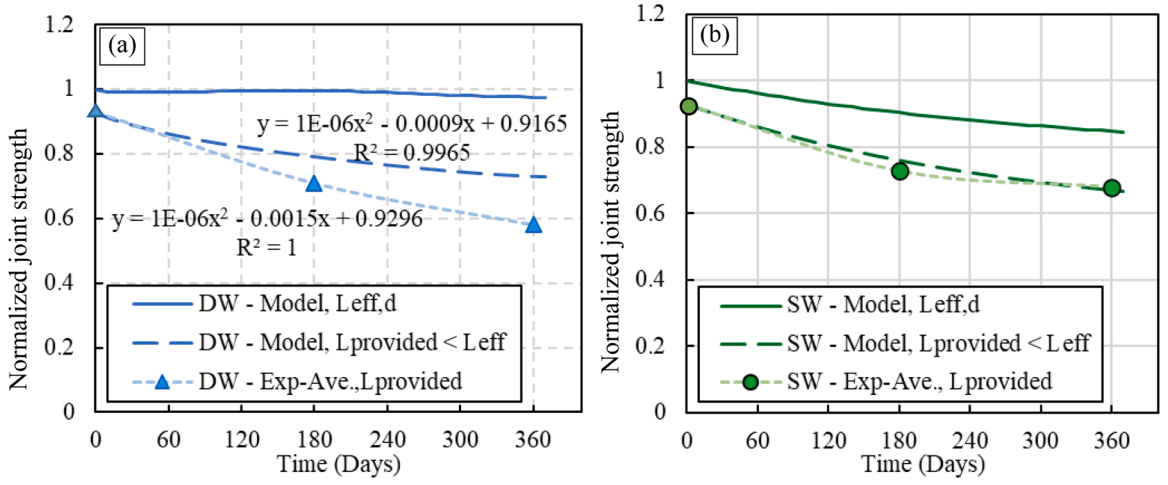

Fig. 9. Comparison of experimental and model predicted joint strength degradation over time (a) DW condition (b) SW condition.

a seawater condition was mainly dominated by the degradation properties of the adhesive. Thus, the designers should focus more on this matter at the preliminary design stage. However, extra precautions against galvanic corrosion might be needed for the durability of the bond.

In DW condition (Fig. 9(a)), the model predicted bond strength curve when provided with L_{eff} predicts no bond degradation throughout the exposure period. The reason is the decrement in the stress concentrations in the joint induced due to the plasticization effect of the adhesive with the absorption of water. On the contrary to SW immersion, a gap was observed in the curves related to $L_{Provided}<L_{eff}$ (Fig. 9(b)) which indicates an additional bond strength reduction due to steel-adhesive interface degradation. By analysing these plots, a primitive theoretical relationship between adhesive failure and interface degradation could be derived as follows.

At a time (t) where $0 < t \leq 365$ days and $2E_o t_o < E_i t_i$;.

$$F_{ult} = F_{adh} + F_{int}$$

Where F_{ult} is the ultimate bond capacity, F_{adh} is the bond capacity of the degraded adhesive and $F_{int}$is the adhesion bond capacity of the degraded interface.

If F_{adh} was expressed as a percentage of F_{ult}; $F_{adh} = n * F_{ult}$.

The factor "n" depends on the surface energy of the substrates and its value was determined from the trendlines of the bond strength degradation curves in Fig. 9(a).

$$n = \frac{1E-06\ t^2 - 0.0009.t + 0.9165}{1E-06\ t^2 - 0.0015.t + 0.9296} = 0.0012.t + 0.9491$$

$$F_{int} = F_{ult} - F_{adh} = F_{ult} - n * F_{ult} = (1-n)\ F_{ult} = (0{\cdot}0509 - 0.0012{\cdot}t)\ F_{ult}$$

$$\text{Thus, } F_{int} \Big/ F_{adh} = \frac{(0.0509 - 0.0012.t)F_{ult}}{(0.0012.t + 0.9491)F_{ult}} = -0.009.t + 0.0395 \approx -0.009 * t = -0.9\% * t$$

According to the above-mentioned derivation, the effect of long-term joint strength degradation due to interface degradation is approximately 1% of the contribution from the adhesive degradation, at a time (t). In the present study, since the surface roughening was achieved by grinding this relationship may be valid only for such manually ground steel surface conditions. Thus, to minimize the interface failure in a DW condition, bonded joints should be provided with an adequate bond length as suggested in Section 4.1 along with a better surface treatment process.

5. Conclusions

Both double strap joint specimens and adhesive coupons were subjected to different exposure conditions for up to a year. Prolonged immersion in distilled water, seawater and cyclic exposure to seawater conditions were considered. The bond strength degradation, strain variation and failure modes were experimentally evaluated. The following conclusions were made:

1. The material testing results showed higher degradation rates for adhesive strength and elastic modulus in distilled water immersed conditions compared to seawater immersion in 360 days.
2. The bond strength degradation results over the exposure time showed the highest degradation rate of about 63% in cyclic exposure conditions. The residual joint strength capacities were similar for both SW and DW conditions for up to 6 months. After 6 months, a negligible bond strength degradation in SW condition was observed and the specimens exposed in DW condition degraded further up to 40%.
3. Special attention should be given to providing adequate bond length in the specimens exposed to long term environmental conditions since the required bond length increases with the exposure duration and environmental condition due to strength degradation. In the current study, required bond lengths at one side of the joint in SW condition and DW condition were found to be 160 mm and 170 mm, respectively. Based on the current study, two equations were developed to calculate the required bond length in saltwater and distilled water immersion and those are in good agreement with current and previous test results.
4. A theoretical model was developed using the concept in the Hart-Smith model to predict the long-term bond characteristics under long term exposure to DW and SW conditions. The model results were in good agreement with the tested results. This model can effectively be used to determine the required CFRP bond length and performance in SW and DW conditions.
5. The theoretical analysis confirmed that the cohesive failure mode could be ensured for both DW and SW moisture conditions if the above-mentioned effective bond lengths were provided along with a proper surface treatment method. The service performance of specimens immersed in SW was mostly dependent on the adhesive properties while the DW conditioned specimens were affected by both adhesive and adhesion degradation.
6. It is identified that the effect of long-term joint strength degradation due to interface degradation is approximately 1% of the contribution from adhesive degradation, at a time (t).

Declaration of Competing Interest

The authors declare that they have no known competing financial interests or personal relationships that could have appeared to influence the work reported in this paper.

Data availability

The raw/processed data required to reproduce these findings cannot be shared at this time as the data also forms part of an ongoing study.

Acknowledgements

The authors would like to express their sincere gratitude towards the staff at the building materials and the structural testing laboratories, Department of Civil Engineering, University of Moratuwa. The Senate Research Commitee, University of Moratuwa, Sri Lanka is greatly acknowledged for arranging the necessary financial support (Grant No: SRC/LT/2019/21).

References

[1] E.R.K. Chandrathilaka, U.N.D. Perera, J.C.P.H. Gamage, Bond slip models for corroded steel – CFRP double strap jointsstrap joints, in: Proceedings of the Sixth Int. Symp. Adv. Civ. Environ. Eng. Pract. Sustain. Dev., 2018.
[2] M.H. Kabir, S. Fawzia, T.H.T. Chan, J.C.P.H. Gamage, J.B. Bai, Experimental and numerical investigation of the behaviour of CFRP strengthened CHS beams subjected to bending, Eng. Struct. 113 (2016) 160–173, https://doi.org/10.1016/j.engstruct.2016.01.047.
[3] M. Elchalakani, A. Karrech, H. Basarir, M.F. Hassanein, S. Fawzia, Thin-walled structures CFRP strengthening and rehabilitation of corroded steel pipelines under direct indentation, Thin Walled Struct. 119 (2017) 510–521, https://doi.org/10.1016/j.tws.2017.06.013.
[4] E.R. Chandrathilaka, G.J.C.P.H. Fire, Performance of CFRP Strengthened Steel I Beams Cured at Elevated Temperature, Springer, Singapore, 2019.
[5] E.R.K. Chandrathilaka, J.C.P.H. Gamage, S. Fawzia, Numerical modelling of bond shear stress slip behavior of CFRP/steel composites cured and tested at elevated temperature, Compos. Struct. 212 (2019) 1–10, https://doi.org/10.1016/j.compstruct.2019.01.002.
[6] E.R.K. Chandrathilaka, J.C.P.H. Gamage, S. Fawzia, Mechanical characterization of CFRP / steel bond cured and tested at elevated temperature, Compos. Struct. 207 (2019) 471–477, https://doi.org/10.1016/j.compstruct.2018.09.048.
[7] U.N.D. Perera, J.C.P.H. Gamage, Bond performance of cfrp/steel composites: state –of-the-art- review, in: Proceedings of the Seventh Int. Conf. Sustain. Built Environ., Kandy, Sri Lanka, 2016. ⟨http://dl.lib.mrt.ac.lk/handle/123/12613⟩.
[8] M. Heshmati, R. Haghani, M. Al-Emrani, Durability of CFRP/steel joints under cyclic wet-dry and freeze-thaw conditions, Compos. Part B Eng. 126 (2017) 211–226, https://doi.org/10.1016/j.compositesb.2017.06.011.
[9] M.R. Bowditch, The durability of adhesive joints in the presence of water, Int. J. Adhes. Adhes. 16 (1996) 73–79.
[10] J. Zhou, J.P. Lucas, Hygrothermal effects of epoxy resin. Part I :the nature of water in epoxy, Polymer 40 (1999) 5505–5512.
[11] M. Dawood, S. Rizkalla, Environmental durability of a CFRP system for strengthening steel structures, Constr. Build. Mater. 24 (2010) 1682–1689, https://doi.org/10.1016/j.conbuildmat.2010.02.023.
[12] J. Li, J. Xie, F. Liu, Z. Lu, A critical review and assessment for FRP-concrete bond systems with epoxy resin exposed to chloride environments, Compos. Struct. 229 (2019), 111372, https://doi.org/10.1016/j.compstruct.2019.111372.
[13] T.C. Nguyen, Y. Bai, X.L. Zhao, R. Al-Mahaidi, Durability of steel/CFRP double strap joints exposed to sea water, cyclic temperature and humidity, Compos. Struct. 94 (2012) 1834–1845, https://doi.org/10.1016/j.compstruct.2012.01.004.
[14] M. Heshmati, R. Haghani, M. Al-emrani, Durability of bonded FRP-to-steel joints: effects of moisture, de-icing salt solution, temperature and FRP type, Compos. Part B 119 (2017) 153–167, https://doi.org/10.1016/j.compositesb.2017.03.049.
[15] Y. Pang, G. Wu, H. Wang, Z. Su, X. He, Experimental study on the bond behavior of CFRP-steel interfaces under quasi-static cyclic loading, Thin Walled Struct. 140 (2019) 426–437, https://doi.org/10.1016/j.tws.2019.03.060.
[16] D. Borrie, S. Al-Saadi, X.-L. Zhao, R.K.S. Raman, Y. Bai, Bonded CFRP/steel systems, remedies of bond degradation and behaviour of CFRP repaired steel: an overview, Polymers 13 (2021), https://doi.org/10.3390/polym13091533.
[17] H.U. Sajid, R. Kiran, Influence of corrosion and surface roughness on wettability of ASTM A36 steels, J. Constr. Steel Res. 144 (2018) 310–326, https://doi.org/10.1016/j.jcsr.2018.01.023.
[18] M.R.E.F. Ariyachandra, J.C.P.H. Gamage, R. Al-Mahaidi, R. Kalfat, Effects of surface roughness and bond enhancing techniques on flexural performance of CFRP/concrete composites, Compos. Struct. 178 (2017) 476–482, https://doi.org/10.1016/j.compstruct.2017.07.028.
[19] M.A.G. Silva, H. Biscaia, P. Ribeiro, On factors affecting CFRP-steel bonded joints, Constr. Build. Mater. 226 (2019) 360–375, https://doi.org/10.1016/j.conbuildmat.2019.06.220.
[20] O. Russian, S. Khan, A. Belarbi, M. Dawood, Effect of surface preparation technique on bond behavior of CFRP-steel double-lap joints: experimental and numerical studies, Compos. Struct. 255 (2021), 113048, https://doi.org/10.1016/j.compstruct.2020.113048.
[21] J. Teng, D. Fernando, T. Yu, X.L. Zhao, Treatment of steel surfaces for effective adhesive bonding, in: Proceedings of the Fifth Int. Conf. FRP Compos. Civ. Eng., Adv. FRP Compos. Civ. Eng. (2011) 865–868.
[22] F.M. Lucas, J.C. Paulo, R.D. Adams, J.K. Spelt, Analytical models of adhesively bonded joints—part I: literature survey, Int. J. Adhes. Adhes. 29 (2009) 319–330, https://doi.org/10.1016/j.ijadhadh.2008.06.005.
[23] F.M. Lucas, J.C. Paulo, R.D. Adams, A. Wang, J.K. Spelt, Analytical models of adhesively bonded joints—Part II: Comparative study, Int. J. Adhes. Adhes. 29 (2009) 331–341, https://doi.org/10.1016/j.ijadhadh.2008.06.007.
[24] Technical datasheet, X-Wrap C300, High Strength Carbon Fiber Fabric for Structural Strengthening, (n.d.). ⟨http://www.x-calibur.us⟩. (Accessed 5 December 2019).
[25] Araldite 420 A/B Epoxy Adhesive, (n.d.).
[26] ASTM, ASTM D 638 - 02a Standard Test Method for Tensile Properties of Plastics, West Conshohocken, PA, 2003.
[27] ASTM D 3039/D 3039M - 00 Standard Test Method for Tensile Properties of Polymer Matrix Composite Materials, West Conshohocken, PA, 2000.
[28] ASTM, A.S.T.M. A 370–08a Standard Test Methods and Definitions for Mechanical Testing of Steel Products, West Conshohocken, PA, 2008.
[29] X.L. Zhao, L. Zhang, State-of-the-art review on FRP strengthened steel structures, Eng. Struct. 29 (2007) 1808–1823, https://doi.org/10.1016/j.engstruct.2006.10.006.
[30] L.S. Lee, Rehabilitation and service life estimation of bridge superstructures, in: Serv. Life Estim. Ext. Civ. Eng. Struct., (2011), 117–142. ⟨https://doi.org/10.1533/9780857090928.1.117⟩.
[31] S.H. Xia, J.G. Teng, Behaviour of FRP-to-Steel Bonded Joints, in: Proceedings of the Int. Symp. Bond Behav. FRP Struct. (BBFS 2005), (2005), 411–418.
[32] M.A. Abanilla, Y. Li, V.M. Karbhari, Durability characterization of wet layup graphite/epoxy composites used in external strengthening, Compos. Part B Eng. 37 (2006) 200–212, https://doi.org/10.1016/j.compositesb.2005.05.016.
[33] K.K. Phani, N.R. Bose, Temperature dependence of hydrothermal ageing of CSM-laminate during water immersion, Compos. Sci. Technol. 29 (1987) 79–87.
[34] L.J. Hart-Smith, Adhesive-bonded double lap joints, in: Technical report NASA CR-112235, Long Beach, California, USA, 1973.
[35] T.C. Nguyen, Y. Bai, X.L. Zhao, R. Al-Mahaidi, Mechanical characterization of steel/CFRP double strap joints at elevated temperatures, Compos. Struct. 93 (2011) 1604–1612, https://doi.org/10.1016/j.compstruct.2011.01.010.